Journal of Chemical&Engineering Data

pubs.acs.org/jced Article

Perfluorinated Alcohols at High Pressure: Experimental Liquid Density and Computer Simulations

Diogo Machacaz, Tiago M. Eusébio, Cátia Guarda, Gonçalo M. C. Silva, Pedro Morgado, Luís F. G. Martins, José N. A. Canongia Lopes, and Eduardo J. M. Filipe*

Cite This: https://doi.org/10.1021/acs.jced.2c00410 Read Online

ACCESS | Metrics & More | Article Recommendations | Supporting Information

ABSTRACT: The liquid density of five liquid 1*H*,1*H*-perfluorinated alcohols ($CF_3(CF_2)_{n-1}CH_2OH$ n = 2, 3, 4, 5, 6) was measured as a function of pressure (0.1−70 MPa) and temperature (293.15−313.15 K). The corresponding isothermal compressibility and isobaric thermal expansivity coefficients were calculated from the experimental data. The results are compared with data from the literature for the equivalent hydrogenated alcohols. Atomistic molecular dynamics simulations were also performed, providing molecular-level insight into the experimental results, in particular about the H-bond network of the perfluorinated alcohols and the effect of pressure on the organization of the liquid.

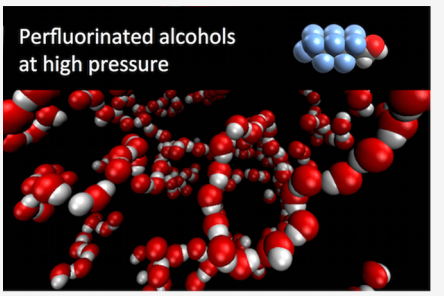

1. INTRODUCTION

Perfluorinated alcohols, carboxylic acids, and their salts are industrially important substances and find applications in numerous products from textile surface agents and fire-fighting foams to detergents and paints and in the production of fluorinated polymers.[1] Since perfluorinated chains are more hydrophobic than hydrogenated chains, they display an enhanced amphiphilic character compared to their hydrogenated analogues and are known to be more acidic. However, in spite of their interesting and useful properties, these substances tend to accumulate in the environment due to their chemical stability and have become significant pollutants. The availability of accurate thermodynamic properties is thus of utmost importance to develop remediation strategies.

Perfluorinated alcohols are highly fluorinated molecules with a terminal OH group and general formula $CF_3(CF_2)_{n-1}(CH_2)_mOH$ (often abbreviated as n/m FTOH). Two major groups of perfluorinated alcohols can be considered: "odd perfluorinated alcohols" when m = 1 and "even perfluorinated alcohols" when m = 2. Alcohols with m = 0 are not chemically stable. In this work, we have studied odd perfluorinated alcohols (1*H*,1*H*-perfluoroalkanols or n:1 FTOH).

This work is part of a project in which experimental measurements, molecular dynamics (MD) simulations, and theoretical calculations are simultaneously used to study the properties of perfluorinated substances. We recently reported new experimental data, computer simulations, and theoretical predictions of vapor pressures, liquid densities, and surface tensions of pure perfluorinated alcohols,[2,3] as well as diffusion coefficients in aqueous solutions.[4,5]

The tendency of alcohol molecules to form H-bonds sequentially, creating a flexible network of linear, cyclic, and ramified (lasso) aggregates of various sizes is well known.[6] The apolar alkyl chains are then stored the best possible way within the space between the H-bond network. The average number of alcohol molecules involved in each type of aggregate varies strongly for each specific alcohol. The bulk structure of liquid alcohols is thus a highly organized micro-heterogeneous environment.

Mixtures of fluorinated and hydrogenated alcohols have also been studied in both the liquid and gaseous phases.[7−12] These mixtures display a very complex behavior when compared with mixtures of hydrogenated alcohols. For example, excess volumes are large and positive, whereas those of mixtures of hydrogenated alcohols are practically zero.[13] We have shown that this complex behavior results from a balance between the formation of a preferential hydrogen bond between the two different alcohols and the weak dispersion forces between the hydrogenated and perfluorinated chains. Indeed, it is well known that perfluorinated and hydrogenated chains are mutually phobic and tend to phase-separate, giving rise to large volumetric,[14] dynamic,[15] and conformational anomalies.[16] This mutual phobicity also leads to inhomogeneities in the fluids and the formation of nano-domains[17] as well as different levels of supramolecular organization.[18−22] In the case

Received: June 25, 2022
Accepted: November 17, 2022

Table 1. CAS Registry Number, Stated Mass Fraction Purity, and Force-Field Model Used in Molecular Dynamics Simulations (MD-FF Model) of the Chemicals Studied

component	CAS reg. no.	supplier	purification method	purity %	analysis method	MD-FF model
CF_3CH_2OH	75-89-8	-				OPLS-AA
$CF_3CF_2CH_2OH$	422-05-9	Apollo Scientific	dried with VWR Prolabo 4 Å molecular sieves	>98	^{1}H NMR	OPLS-AA
$CF_3(CF_2)_2CH_2OH$	375-01-9	Apollo Scientific	dried with VWR Prolabo 4 Å molecular sieves	>98	^{1}H NMR	OPLS-AA
$CF_3(CF_2)_3CH_2OH$	355-28-2	Apollo Scientific	dried with VWR Prolabo 4 Å molecular sieves	>97	^{1}H NMR	OPLS-AA
$CF_3(CF_2)_4CH_2OH$	423-46-1	Apollo Scientific	dried with VWR Prolabo 4 Å molecular sieves	>98	^{1}H NMR	OPLS-AA
$CF_3(CF_2)_5CH_2OH$	375-82-6	Apollo Scientific	dried with VWR Prolabo 4 Å molecular sieves	>97	^{1}H NMR	OPLS-AA

Table 2. Experimental Density[a] as a Function of Pressure and Temperature for 1*H*,1*H*-Perfluoropropan-1-ol ($CF_3CF_2CH_2OH$)

2:1 FTOH									
T = 293.15 K		T = 298.15 K		T = 303.15 K		T = 308.15 K		T = 313.15 K	
p/MPa	ρ/kg m^{-3}	p/MPa	ρ/kg·m^{-3}	p/MPa	ρ/kg·m^{-3}	p/MPa	ρ/kg·m^{-3}	p/MPa	ρ/kg·m^{-3}
0.10	1514.4	0.10	1504.5	0.10	1494.3	0.10	1484.2	0.10	1473.9
0.76	1515.7	0.82	1505.8	0.73	1495.8	0.90	1486.2	0.63	1475.4
3.07	1519.5	2.94	1509.8	2.87	1499.8	3.59	1491.3	3.10	1480.2
4.04	1521.7	3.22	1510.5	3.79	1501.8	3.87	1492.3	6.80	1487.6
6.49	1525.7	6.07	1515.8	6.07	1506.2	10.62	1504.6	7.24	1489.0
6.93	1526.9	6.21	1515.8	7.69	1508.8	10.62	1505.0	9.80	1493.4
10.03	1531.8	10.21	1522.9	10.02	1513.0	14.69	1511.7	10.52	1495.3
10.73	1533.4	10.88	1524.3	11.24	1515.5	16.07	1514.6	13.17	1499.6
13.14	1537.0	13.35	1528.2	13.60	1519.3	20.00	1520.6	16.07	1505.3
16.35	1542.4	15.77	1532.4	16.00	1523.6	22.69	1525.3	20.00	1511.4
20.19	1548.0	19.86	1538.6	20.31	1530.2	26.76	1531.2	26.83	1522.3
23.10	1552.6	22.01	1542.1	22.68	1534.1	29.01	1534.9	29.51	1526.9
27.94	1559.3	26.76	1548.8	26.82	1540.1	36.75	1545.9	33.65	1532.6
29.20	1561.3	29.82	1553.4	29.33	1543.9	40.79	1551.1	37.10	1537.8
33.89	1567.4	34.06	1559.0	33.86	1550.2	43.79	1555.2	40.55	1542.3
35.86	1570.2	36.41	1562.4	36.25	1553.6	48.27	1560.8	43.68	1546.7
40.55	1576.0	40.55	1567.5	40.55	1559.1	50.82	1564.1	47.85	1552.0
43.65	1580.0	43.89	1572.0	43.87	1563.6	54.34	1568.3	50.92	1555.9
47.72	1584.8	47.65	1576.4	48.61	1569.4	57.58	1572.3	55.99	1562.2
50.52	1588.2	50.45	1580.0	50.23	1571.5	63.61	1579.1	61.37	1568.6
54.58	1592.9	55.22	1585.5	55.09	1577.3	69.23	1585.4	63.70	1571.2
57.78	1596.6	57.39	1588.1	56.96	1579.5			68.26	1576.5
61.85	1601.0	61.71	1592.9	61.39	1584.6				
64.06	1603.4	64.42	1596.0	64.15	1587.6				
68.40	1608.2	68.69	1600.6	68.92	1592.9				

[a]Standard uncertainties are $u(T)$ = 0.01 K and $u(p)$ = 0.08 MPa. The expanded relative uncertainty for ρ is $u_r(\rho)$ = 0.002 (k = 2).

of mixtures of hydrogenated and fluorinated alcohols, we have demonstrated that they display nano-segregation.[7−9] Thus, in addition to the previously mentioned network of H-bonds zigzagging throughout the liquid, the simultaneous presence of the mutually phobic alkyl and perfluoroalkyl segments introduces a new important constraint to the organization of the fluid. The result is a highly nano-segregated structure, reflecting the difficult balance between maximizing H-bonding and the tendency to isolate fluorinated from hydrogenated chains. We have also shown that water tends to aggregate along the H-bond network. Emulsions featuring aqueous, hydrogenated, and fluorinated domains are thus formed.

In this work, we report new experimental data for the liquid density of five liquid 1*H*,1*H*-perfluoroalkanols ($CF_3(CF_2)_{n-1}CH_2OH$, n = 2−6) as a function of pressure and temperature. The equation of state, $\rho = f(p,T)$, of the studied perfluorinated alcohols was thus determined. The corresponding isothermal compressibility and isobaric thermal expansivity coefficients were calculated from the experimental data. To the best of our knowledge, these are the first systematic high-pressure data reported for this family of compounds. Together with our previously mentioned papers and that of Costa et al. reporting vapor pressures for the longer odd alcohols ($CF_3(CF_2)_{n-1}CH_2OH$, n = 5−9),[23] these four publications cover the fundamental thermodynamic data for the family of 1*H*,1*H*-perfluorinated alcohols. Finally, atomistic MD simulations were also performed, providing molecular-level insight into the experimental results. From the MD simulations, a detailed quantitative analysis of the H-bond network of the pure perfluorinated alcohols was performed. The influence of pressure on the organization of the alcohols was also analyzed.

2. EXPERIMENTAL SECTION

The characteristics of the 1*H*,1*H*-perfluoroalcohols used ($CF_3(CF_2)_{n-1}CH_2OH$, n = 2−6, abbreviated as n:1 FTOH) are collected in Table 1. All the compounds were dried with

https://doi.org/10.1021/acs.jced.2c00410
J. Chem. Eng. Data XXXX, XXX, XXX−XXX

Table 3. Experimental Density[a] as a Function of Pressure and Temperature for 1*H*,1*H*-Perfluorobutan-1-ol ($CF_3(CF_2)_2CH_2OH$)

3:1 FTOH									
T = 293.15 K		T = 298.15 K		T = 303.15 K		T = 308.15 K		T = 313.15 K	
p/MPa	ρ/kg·m^{-3}	p/MPa	ρ/kg·m^{-3}	p/MPa	ρ/kg·m^{-3}	p/MPa	ρ/kg·m^{-3}	p/MPa	ρ/kg·m^{-3}
0.10	1596.6	0.10	1586.3	0.10	1576.3	0.10	1565.7	0.10	1555.4
2.83	1601.6	0.80	1587.8	0.66	1577.4	1.02	1568.0	0.88	1557.4
4.35	1604.8	2.69	1591.4	2.62	1581.2	3.11	1572.2	3.11	1562.0
6.18	1607.9	4.27	1594.7	4.35	1585.0	4.01	1574.4	4.28	1564.9
7.80	1611.1	6.07	1598.1	6.21	1588.4	6.69	1579.8	6.28	1568.7
9.66	1614.1	6.91	1599.8	7.60	1591.4	6.83	1579.8	7.45	1571.5
10.97	1616.8	9.52	1604.3	9.52	1594.7	9.90	1585.8	9.86	1576.0
13.17	1620.2	10.88	1607.1	10.90	1597.6	10.57	1587.4	10.96	1578.5
15.46	1624.4	12.97	1610.4	12.97	1601.0	13.50	1592.5	12.97	1582.0
19.90	1631.1	16.48	1616.8	15.64	1606.1	15.87	1597.2	16.41	1588.8
22.93	1636.2	20.41	1622.8	20.03	1613.1	19.86	1603.7	19.86	1594.5
26.99	1641.9	22.90	1627.1	23.07	1618.5	23.10	1609.5	22.92	1600.1
29.71	1646.2	27.09	1633.2	26.80	1623.9	26.76	1615.0	26.76	1606.1
33.86	1651.7	30.20	1638.1	30.29	1629.5	29.98	1620.4	29.58	1611.0
37.40	1656.8	33.72	1642.8	33.79	1634.4	33.65	1625.6	34.00	1617.5
40.55	1660.8	36.62	1647.2	35.86	1637.7	36.89	1630.7	37.10	1622.5
44.10	1665.6	40.55	1652.3	40.65	1644.1	40.55	1635.6	40.65	1627.4
48.13	1670.5	42.68	1655.4	44.06	1648.9	43.75	1640.3	47.44	1637.0
50.01	1673.1	47.65	1661.7	47.58	1653.4	48.03	1645.9	51.03	1641.9
54.45	1678.4	51.07	1666.2	50.42	1657.3	50.54	1649.4	54.99	1647.0
57.74	1682.4	54.34	1670.1	54.92	1662.8	54.54	1654.4	57.57	1650.4
61.74	1687.0	57.50	1674.0	57.24	1665.8	61.92	1663.6	61.23	1655.0
64.40	1690.1	62.02	1679.4	61.23	1670.6	62.81	1664.7	63.73	1657.9
68.15	1694.4	64.39	1682.1	64.02	1673.9	69.02	1672.0	69.35	1664.6
		68.12	1686.5	68.12	1678.7				

[a]Standard uncertainties are $u(T)$ = 0.01 K and $u(p)$ = 0.08 MPa. The expanded relative uncertainty for ρ is $u_r(\rho)$ = 0.002 (k = 2).

VWR Prolabo 4 Å molecular sieves to a maximum water content of 500 μg/g (analyzed by Karl-Fischer Coulometry).

The densities at high pressure were measured in an Anton Paar DMA HP vibrating tube densimeter external cell, connected to a DMA 5000 densimeter. The sample is thermostated by an internal temperature control system that is stable at $T \pm 0.001$ K. The measuring cell is connected to a high-pressure generator and to a Setra 280E pressure transducer, which has an accuracy of 0.08 MPa. The system was calibrated in vacuum over the whole range of measurement temperatures and with water, toluene, and dichloromethane in the whole range of temperatures and pressures, giving a total of 737 calibration points; the average of the absolute residuals of the overall fit in relation to the literature data[24−26] for the calibrating fluids was 3×10^{-2} kg m^{-3}, and the individual deviations were always smaller than 2×10^{-1} kg m^{-3}. The cleanliness of the measurement cell was verified at the beginning of each series of measurements by checking the measured density of air.

3. SIMULATION DETAILS

MD simulations were carried out to obtain molecular-level information on the behavior of the studied systems using an all-atom force field based on OPLS-AA.[27] For the perfluoroalkyl segments of the molecules, the OPLS-AA parameters from Watkins and Jorgensen[28] were used, while the $-CF_2CH_2OH$ segment was modeled with the parameters developed by Duffy for 1:1 FTOH.[25,26] The full set of parameters has been already presented in previous publications.[2,3]

The simulations were performed for systems consisting of 300 molecules in cubic simulation boxes with periodic boundary conditions using the Gromacs 5.0.7 software[29] in the NPT ensemble. Box lengths for the equilibrated systems ranged from ∼3.2 nm for 1:1 FTOH at 100 MPa to ∼4.6 nm for 6:1 FTOH at 0.1 MPa. The temperature and pressure were kept constant using the Nosé−Hoover thermostat and the Parrinello−Rahman barostat, with relaxation constants of 0.5 and 10 ps, respectively. All bonds involving hydrogen atoms were constrained to their equilibrium lengths using the LINCS algorithm, and a 2 fs timestep was used for the integration of the equations of motion. A cutoff of 14 Å was applied to both the dispersive and electrostatic potentials. The particle-mesh Ewald method was used to account for the electrostatic interactions beyond the cutoff distance, and standard analytical tail corrections to the dispersive terms were applied to both energy and pressure. At least 5 ns of simulation time was considered as the equilibration time, with a further 15 ns used for property averaging. Temperature, density, and all components of the potential energy were monitored to confirm that these properties reached equilibrium within the equilibration time and that no significant variation or drift occurred during the production stage. Volume and potential energy plots as a function of time for a typical simulation can be found in Figure S1. The uncertainties u of the simulated properties were estimated dividing the production run in five equal blocks and calculating the standard deviation of the block averages.

https://doi.org/10.1021/acs.jced.2c00410
J. Chem. Eng. Data XXXX, XXX, XXX−XXX

Table 4. Experimental Density[a] as a Function of Pressure and Temperature for 1*H*,1*H*-Perfluoropentan-1-ol ($CF_3(CF_2)_3CH_2OH$)

4:1 FTOH									
T = 293.15 K		T = 298.15 K		T = 303.15 K		T = 308.15 K		T = 313.15 K	
p/MPa	ρ/kg·m^{-3}	p/MPa	ρ/kg·m^{-3}	p/MPa	ρ/kg·m^{-3}	p/MPa	ρ/kg·m^{-3}	p/MPa	ρ/kg·m^{-3}
0.10	1667.3	0.10	1657.1	0.10	1646.8	0.10	1636.6	0.10	1626.1
0.83	1668.7	0.90	1658.6	0.69	1648.0	0.90	1638.4	0.90	1627.9
3.80	1673.9	3.40	1663.3	3.45	1653.4	3.25	1643.5	3.31	1633.3
3.83	1674.6	3.66	1664.1	3.80	1654.4	3.62	1643.6	3.52	1633.2
6.90	1679.7	6.76	1669.7	6.90	1660.5	6.90	1650.2	6.76	1640.4
7.45	1681.3	10.07	1675.8	6.97	1660.3	6.90	1650.8	7.18	1640.8
10.00	1685.3	10.62	1677.3	10.69	1667.2	10.48	1657.7	10.76	1647.9
10.55	1686.8	13.66	1682.1	10.71	1667.7	10.76	1657.6	10.97	1648.8
13.52	1691.3	15.59	1685.9	14.07	1673.3	13.66	1663.0	14.11	1654.2
16.69	1697.1	20.76	1693.8	20.28	1683.8	16.41	1668.5	15.62	1657.6
19.86	1701.7	22.55	1697.1	22.41	1687.7	21.00	1675.9	20.21	1665.2
23.31	1707.5	27.72	1704.6	27.31	1695.0	23.31	1680.1	23.05	1670.6
26.93	1712.5	34.00	1713.9	28.89	1697.9	28.27	1687.6	27.20	1676.9
29.41	1716.4	35.79	1716.6	34.34	1705.6	29.55	1690.0	30.13	1682.1
33.86	1722.5	41.51	1724.2	35.72	1707.9	33.75	1696.0	34.41	1688.2
36.82	1726.8	43.34	1726.9	41.44	1715.7	36.31	1700.0	36.06	1691.2
40.55	1731.6	48.13	1733.0	42.96	1717.9	41.58	1707.3	41.27	1698.5
43.10	1735.1	50.27	1735.8	48.51	1725.2	43.17	1709.7	43.37	1701.7
48.41	1741.7	55.71	1742.7	49.37	1726.4	47.79	1716.0	48.27	1708.4
50.27	1744.2	56.40	1743.5	55.02	1733.6	50.54	1719.7	50.30	1711.2
55.02	1750.0	62.23	1750.6	56.89	1736.0	54.75	1725.2	54.89	1717.3
56.80	1752.2	63.23	1751.7	62.37	1742.8	57.32	1728.4	56.99	1720.0
62.61	1759.1	69.85	1759.6	64.08	1744.7	61.78	1734.0	61.78	1726.1
63.41	1760.0			69.50	1751.2	62.26	1734.5	63.18	1727.8
68.61	1766.1					69.16	1742.9	68.57	1734.3

[a]Standard uncertainties are $u(T)$ = 0.01 K and $u(p)$ = 0.08 MPa. The expanded relative uncertainty for ρ is $u_r(\rho)$ = 0.002 (k = 2).

4. RESULTS AND DISCUSSION

The liquid density of the five studied 1*H*,1*H*-perfluorinated alcohols was determined as a function of temperature and pressure. Isothermal curves were obtained between 293.15 and 313.15 K in 5 K intervals and from atmospheric pressure up to 70 MPa. In the case of 6:1 FTOH, it was only possible to obtain the full isotherm at 308.15 and 313.15 K since at the lower temperatures, the compound solidified during the compression. For this reason, only the values at atmospheric pressure are reported between 293.15 and 303.15 K. At least 25 data points were taken along each isotherm for a total of approximately 130 data points for each substance. The data were fitted with the modified Tait equation[30]

$$\frac{1}{\rho(p,\,T)} = \frac{1}{\rho_0(T)} + A(T)\ln\left(\frac{B(T)+p_0}{B(T)+p}\right) \quad (1)$$

where $\rho_0(T)$, $A(T)$, and $B(T)$ are the fitting parameters. $\rho_0(T)$ stands for the density at the reference pressure p_0 = 0.101325 MPa and is given by $\rho_0(T) = \sum_{i=0}^{2}\rho_{0i}T^i$, $A(T)$ is given by $A(T) = \sum_{i=0}^{2}A_iT^i$, and $B(T)$ is given by $B(T) = \sum_{i=0}^{2}B_iT^i$. The fitting coefficients for the five compounds are presented in Table 7, along with the standard deviation of the fit, calculated as

$$\sigma = \sqrt{\frac{\sum_{i=1}^{n}(\rho_{exp} - \rho_{calc})^2}{n}} \quad (2)$$

where n is the number of experimental points. The full set of experimental data is reported in Tables 2−6.

The values at atmospheric pressure are compared with results from the literature,[31−36] in particular from our group,[2,3] in Figures S2−S12. With the exception of the data from Denda et al.,[33] Johnson and Dettre,[34] and Rochester and Symonds[35] for 2:1 FTOH at 298.15 K and Hashemi et al.[36] for 3:1 FTOH

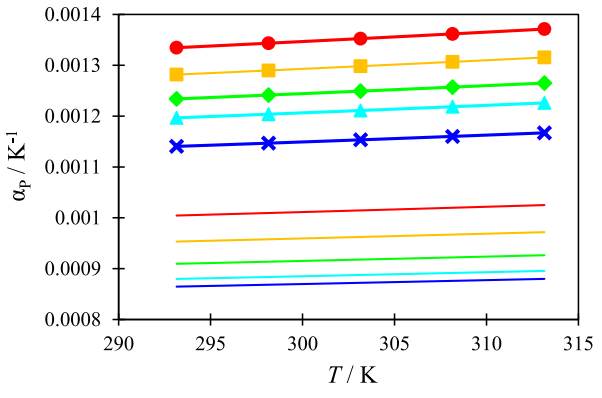

Figure 1. Isobaric thermal expansion coefficients at atmospheric pressure as a function of temperature for the studied 1*H*,1*H*-perfluorinated alcohols and selected hydrogenated alcohols of similar chain lengths (1-propanol, 1-butanol, 1-pentanol, 1-hexanol, and 1-heptanol, as solid lines). 2:1 FTOH (red ●), 3:1 FTOH (orange ■), 4:1 FTOH (green ♦), 5:1 FTOH (aqua blue ▲), and 6:1 FTOH (blue ×). The results for the hydrogenated alcohols were calculated from the density correlations of Cibulka.[25,26]

https://doi.org/10.1021/acs.jced.2c00410
J. Chem. Eng. Data XXXX, XXX, XXX−XXX

Table 5. Experimental Density[a] as a Function of Pressure and Temperature for 1*H*,1*H*-Perfluorohexan-1-ol ($CF_3(CF_2)_4CH_2OH$)

5:1 FTOH									
T = 293.15 K		T = 298.15 K		T = 303.15 K		T = 308.15 K		T = 313.15 K	
p/MPa	ρ/kg·m−3	p/MPa	ρ/kg·m−3	p/MPa	ρ/kg·m−3	p/MPa	ρ/kg·m−3	p/MPa	ρ/kg·m−3
0.09	1720.8	0.10	1710.7	0.10	1700.5	0.10	1690.2	0.10	1679.9
0.89	1722.3	0.55	1711.6	3.17	1705.9	0.89	1691.8	3.31	1686.7
3.31	1726.9	2.69	1715.1	3.58	1707.4	2.89	1695.4	3.79	1687.0
3.38	1726.1	3.31	1716.9	7.03	1714.0	3.93	1698.0	7.31	1694.1
6.07	1731.9	6.31	1721.9	9.80	1718.9	6.62	1703.3	10.48	1700.8
7.03	1732.9	6.48	1722.8	9.93	1718.6	6.75	1703.0	10.75	1700.7
9.86	1738.5	10.48	1729.8	13.65	1725.2	10.34	1709.7	14.61	1707.8
10.55	1739.0	10.62	1729.6	15.86	1729.4	10.68	1711.0	16.41	1711.5
13.82	1744.6	13.52	1734.7	20.82	1737.1	14.34	1716.8	20.23	1717.6
16.45	1749.4	15.99	1739.1	23.32	1741.4	15.03	1718.6	22.61	1722.0
20.34	1755.1	20.08	1745.4	27.03	1746.9	20.13	1726.8	27.23	1729.2
22.96	1759.4	23.30	1750.5	29.58	1751.0	21.79	1729.8	29.51	1733.1
27.23	1765.3	26.82	1755.8	34.54	1758.0	27.09	1738.0	34.54	1740.6
29.99	1769.7	34.33	1766.7	36.06	1760.4	28.82	1741.0	35.99	1742.9
34.33	1775.5	36.68	1769.8	41.50	1767.7	33.71	1748.1	41.30	1750.6
37.09	1779.4	41.57	1776.7	43.09	1770.1	36.95	1753.0	42.47	1752.3
41.33	1784.9	43.16	1778.5	48.12	1776.7	41.57	1759.4	47.43	1759.1
43.64	1788.0	48.12	1785.2	50.12	1779.3	43.50	1762.1	49.78	1762.3
48.12	1793.6	48.93	1785.9	54.54	1784.9	48.61	1769.0	55.02	1769.3
49.78	1795.7	54.60	1793.4	56.26	1787.1	50.54	1771.6	55.57	1770.0
55.43	1802.8	55.78	1794.5	62.40	1794.8	55.43	1778.0	62.02	1778.0
56.40	1803.9	61.36	1801.7	63.15	1795.5	57.05	1779.9	62.26	1778.4
62.62	1811.4	63.49	1804.0	68.67	1802.2	61.77	1786.0	68.67	1786.1
63.42	1812.3	68.46	1810.1			62.26	1786.4		
68.81	1818.7					68.39	1793.9		

[a]Standard uncertainties are $u(T)$ = 0.01 K and $u(p)$ = 0.08 MPa. The expanded relative uncertainty for ρ is $u_r(\rho)$ = 0.002 (k = 2).

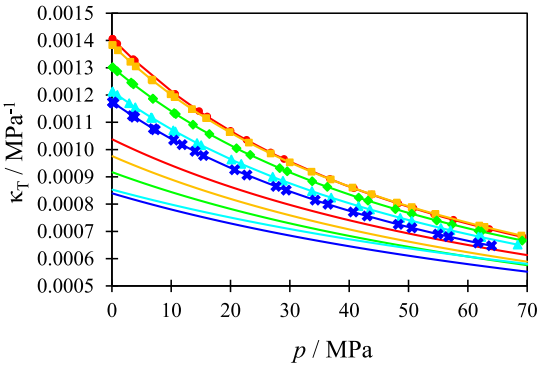

Figure 2. Isothermal compressibility coefficients at 308.15 K as a function of pressure for the studied 1*H*,1*H*-perfluorinated alcohols and selected hydrogenated alcohols of similar chain lengths (1-propanol, 1-butanol, 1-pentanol, 1-hexanol, and 1-heptanol, as solid lines). 2:1 FTOH (red ●), 3:1 FTOH (orange ■), 4:1 FTOH (green ♦), 5:1 FTOH (aqua blue ▲), and 6:1 FTOH (blue ×). The results for the hydrogenated alcohols were calculated from the density correlations of Cibulka.[25,26]

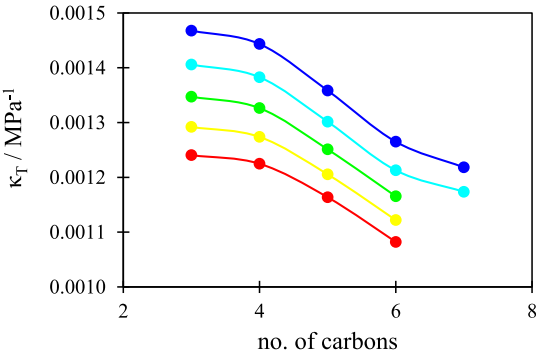

Figure 3. Isothermal compressibility coefficients at atmospheric pressure as a function of the number of carbon atoms: 293.15 K (red ●), 298.15 K (orange ●), 303.15 K (green ●), 308.15 K (aqua blue ●), and 313.15 K (blue ●).

at 293.15 K, all deviations are below 0.6% and do not correlate with the density or chain length of the compounds. As previously discussed, part of these differences, although very small, may be related to the existence of unavoidable isomeric impurities, which are known to be common in different batches of perfluorinated solvents.[2] It should be noted that data from Denda et al., Johnson and Dettre, Rochester and Symonds, and Hashemi et al. are reported at a single temperature and display much larger deviations than all other authors, including the present work. Data as a function of pressure could only be compared for 2:1 FTOH at 298.15 K with the results of Matsuo et al.[32] As seen in Figures S13 and S14, all deviations are below 0.2%..

The isobaric thermal expansion coefficient can be obtained from the dependence of density with temperature at constant pressure

$$\alpha_p = \frac{-1}{\rho}\left(\frac{\partial \rho}{\partial T}\right)_p \quad (3)$$

https://doi.org/10.1021/acs.jced.2c00410
J. Chem. Eng. Data XXXX, XXX, XXX−XXX

Table 6. Experimental Density[a] as a Function of Pressure and Temperature for 1*H*,1*H*-Perfluoroheptan-1-ol ($CF_3(CF_2)_5CH_2OH$)

6:1 FTOH					
T = 293.15 K		T = 308.15 K		T = 313.15 K	
p/MPa	ρ/kg·m^{-3}	p/MPa	ρ/kg·m^{-3}	p/MPa	ρ/kg·m^{-3}
0.10	1744.5	0.10	1714.8	0.10	1704.7
		0.11	1715.0	0.31	1705.3
T = 298.15 K		0.34	1715.5	3.48	1711.9
p/MPa	ρ/kg·m^{-3}	3.45	1721.7	3.50	1711.5
0.10	1734.9	3.83	1722.2	6.13	1717.1
		6.98	1728.2	6.96	1718.3
T = 303.15 K		7.31	1729.1	10.41	1725.2
p/MPa	ρ/kg·m^{-3}	10.41	1734.8	10.44	1724.8
0.10	1725.0	11.82	1737.0	14.13	1731.4
		13.99	1740.8	15.92	1735.0
		15.44	1743.6	20.41	1742.2
		20.68	1751.9	23.27	1747.2
		22.76	1755.6	26.75	1752.5
		27.65	1762.9	28.68	1755.7
		29.37	1765.7	33.92	1763.3
		34.26	1772.6	36.20	1766.8
		36.40	1775.9	42.06	1775.0
		40.68	1781.7	42.61	1775.9
		43.02	1785.1	48.99	1784.5
		48.26	1791.9	50.19	1786.1
		50.55	1795.0	55.57	1793.1
		54.95	1800.5	57.29	1795.1
		56.74	1802.8	62.53	1801.6
		61.71	1808.8	63.08	1802.1
		63.98	1811.4		

[a]Standard uncertainties are $u(T)$ = 0.01 K and $u(p)$ = 0.08 MPa. The expanded relative uncertainty for ρ is $u_r(\rho)$ = 0.002 (k = 2).

Here, the α_p coefficients at atmospheric pressure were obtained by analytical differentiation of the $\rho_0(T)$ fits and are recorded in Figure 1, where they are compared with data for hydrogenated alcohols of similar chain lengths.[37,38] As expected, the values decrease with the chain length of the alcohol and increase with temperature for each compound.

Isothermal compressibility coefficients reflect the dependence of density with pressure

$$\kappa_T = \frac{1}{\rho}\left(\frac{\partial \rho}{\partial p}\right)_T \quad (4)$$

Table 8. Comparison between MD[a] and Experimental (Smoothed Values from Tait Equation) Density Results for the Studied 1*H*,1*H*-Perfluorinated Alcohols ($CF_3(CF_2)_{n-1}CH_2OH$, n = 1, 2, 3, 4, 5, 6)

p/MPa	T/K	MD density ρ_{sim}/kg·m^{-3}	$u(\rho_{sim})$/kg·m^{-3}	exp. density (eq 1) ρ/kg m^{-3}	deviation (%)
1:1 FTOH (Experimental Values from Ref 7)					
0.1	298.15	1386.1	0.4	1381.4	0.3
50	298.15	1452.1	0.2	1448.1	0.3
100	298.15	1498.9	0.3	1494.2	0.3
2:1 FTOH					
0.1	298.15	1505.5	0.4	1504.5	0.1
50	298.15	1585.2	0.3	1579.4	0.4
100	298.15	1637.9	0.3	1630.5	0.5
3:1 FTOH					
0.1	293.15	1613.6	0.8	1596.5	1.1
0.1	298.15	1604.0	0.4	1586.4	1.1
0.1	313.15	1573.0	0.4	1555.6	1.1
50	298.15	1685.3	0.6	1664.9	1.2
100	298.15	1740.4	0.7	1718.7	1.3
4:1 FTOH					
0.1	298.15	1668.8	0.6	1657.1	0.7
50	298.15	1750.5	0.5	1735.6	0.9
100	298.15	1805.9	0.5	1790.4	0.9
5:1 FTOH					
0.1	293.15	1733.2	0.5	1720.8	0.7
0.1	298.15	1721.6	0.9	1710.6	0.6
0.1	313.15	1692.3	0.7	1679.6	0.8
50	298.15	1801.7	0.3	1787.7	0.8
100	298.15	1857.5	0.7	1842.8	0.8
6:1 FTOH					
0.1	298.15	1760.9	0.8	1734.9	1.5

[a]Standard uncertainties for the simulation results are $u(T_{sim})$ = 0.002 K and $u(p_{sim})$ = 0.03 MPa.

In this case, analytical differentiation of the Tait eq 1 is the most direct and accepted way to obtain κ_T. Figure 2 shows the calculated isothermal compressibilities at 308.15 K and as a function of pressure. The 1*H*,1*H*-perfluorinated alcohols display the usual behavior, with compressibility decreasing with pressure and molecular weight within the homologous family. Again, data for hydrogenated alcohols of similar chain lengths are included for comparison. As can be seen, perfluorinated alcohols are more compressible than their hydrogenated analogues at similar temperatures. The same

Table 7. Coefficients for Eq 1, Obtained by Fitting to the Experimental Density Data for the five n:1 FTOH Studied, along with the Standard Deviation of the Fit

	2:1 FTOH	3:1 FTOH	4:1 FTOH	5:1 FTOH	6:1 FTOH[a]
A_0/m^3 kg^{-1}	3.34506×10^{-4}	1.07821×10^{-4}	-2.57526×10^{-4}	-7.74726×10^{-7}	4.64701×10^{-5}
A_1/m^3 kg^{-1} K^{-1}	-1.85431×10^{-6}	-4.28213×10^{-7}	1.96654×10^{-6}	3.37930×10^{-7}	4.20531×10^{-9}
A_2/m^3 kg^{-1} K^{-2}	3.06473×10^{-9}	8.08348×10^{-10}	-3.13417×10^{-9}	-5.59889×10^{-10}	
B_0/MPa	706.356	350.269	−297.616	199.854	250.176
B_1/MPa K^{-1}	−3.68131	−1.38409	2.90749	-1.75204×10^{-1}	-5.85671×10^{-1}
B_2/MPa K^{-2}	5.10836×10^{-3}	1.42945×10^{-3}	-5.62874×10^{-3}	-8.00594×10^{-4}	
ρ_{00}/kg m^{-3}	1886.267	2046.477	2146.744	2221.745	1957.792
ρ_{01}/kg m^{-3} K^{-1}	-5.64057×10^{-1}	−1.05617	−1.24116	−1.38069	4.53941×10^{-1}
ρ_{02}/kg m^{-3} K^{-2}	-2.40317×10^{-3}	-1.63292×10^{-3}	-1.34575×10^{-3}	-1.11910×10^{-3}	-4.03022×10^{-3}
σ/kg m^{-3}	1.6×10^{-1}	1.6×10^{-1}	2.1×10^{-1}	2.3×10^{-1}	1.5×10^{-1}

[a]Range for 6:1 FTOH between 308.15 and 313.15 K.

https://doi.org/10.1021/acs.jced.2c00410
J. Chem. Eng. Data XXXX, XXX, XXX−XXX

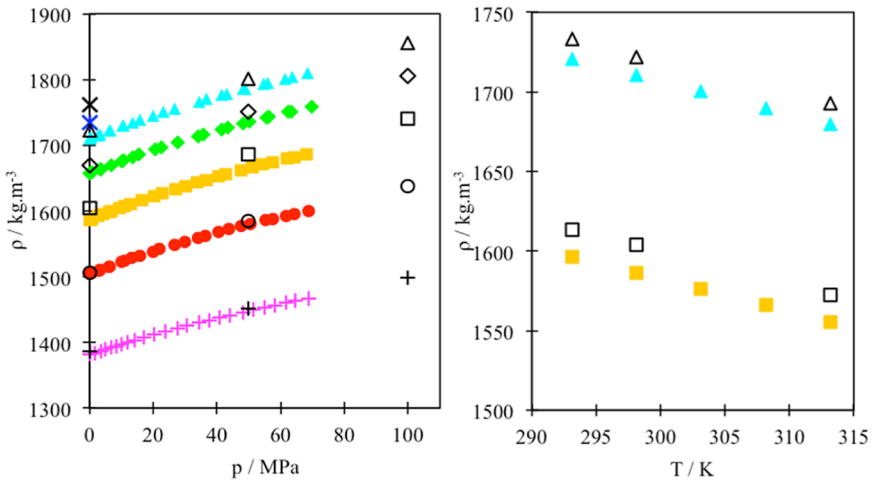

Figure 4. (Left) Liquid densities at 298.15 K as a function of pressure and (right) at 0.1 MPa as a function of temperature for the studied perfluorinated alcohols: colored symbols represent experimental data [1:1 FTOH (pink +),[7] 2:1 FTOH (red ●), 3:1 FTOH (orange ■), 4:1 FTOH (green ♦), 5:1 FTOH (aqua blue ▲), and 6:1 FTOH (blue ×)]; black symbols represent MD simulations results.

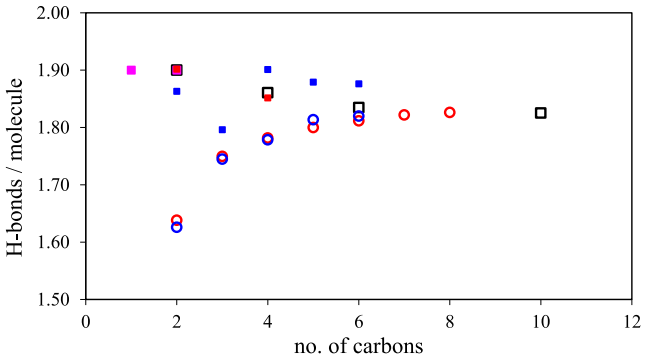

Figure 5. Average number of hydrogen bonds per molecule vs chain length from MD simulations at 298.15 K and 0.1 MPa. Perfluorinated alcohols: blue ○[2] and red ○ (this work); hydrogenated alcohols: pink,■[40] blue ■,[6] red■,[8] and □ (this work).

effect has been previously noticed for alkanes and perfluoroalkanes. However, the increased compressibility due to perfluorination seems to be less important in the case of primary alcohols, probably due to hydrogen bonding. In Figure 3, the isothermal compressibility coefficients at atmospheric pressure are shown as a function of the number of carbon atoms.

The volumetric behavior of the five studied 1*H*,1*H*-perfluorinated alcohols and 2,2,2-trifluoroethanol was also assessed by MD simulations as a function of temperature and pressure. The simulation results are compared with the new experimental data and with our previous results for trifluoroethanol[7] in Table 8 and in Figure 4. As can be seen, the simulation model is able to reproduce quantitatively the experimental densities, with maximum deviations of 1%. The model also reproduces correctly the variation of density with pressure and temperature, lending additional confidence to the validity of the simulation results, even when extrapolating beyond the experimental conditions.

In a previous work,[2] atomistic simulations at 298.15 K and 1 atm for hydrogenated and perfluorinated alcohols have shown that the average number of hydrogen bonds per molecule seems to behave differently along the two families. These findings were further analyzed in the present work and are presented in Figure 5. All intermolecular O−H pairs with a separation smaller than 2.66 Å (the first minimum of the RDF) were considered as hydrogen-bonded. In the case of hydrogenated alcohols, the average number of hydrogen bonds per molecule seems to slightly decrease between 1.90 for methanol and 1.83 for hexanol, becoming constant for the longer alcohols. In the case of the studied perfluorinated alcohols, the average number of hydrogen bonds per molecule gradually increases from 1.63 for 1:1 FTOH, reaching the same limiting value of 1.83 for 7:1 FTOH. This was explained by the predominance of gauche (cis) conformers in perfluorinated alcohols, which favor the formation of intramolecular H-bonds between the hydroxyl H atom and the fluorine atoms. Hydrogenated alcohols, on the contrary, tend to be found in trans (anti) conformation. In perfluorinated alcohols, gauche conformations prevail due to the repulsion between the unshared electron pairs of oxygen and fluorine, the so-called "gauche effect".[39]

The hydrogen bonding aggregation behavior of the 1*H*,1*H*-perfluorinated alcohols was further investigated from the simulation results, analyzing the sizes and types of aggregates present in the bulk liquid. This was done by applying an algorithm,[10] which considers that two molecules are H-bonded and belong to the same aggregate if the hydroxyl hydrogen of one of them is closer than 0.27 nm to the oxygen atom of the other. The size of all aggregates is identified in the analyzed configurations and, for each size, the number of cyclic aggregates (all OH groups in an aggregate have exactly two neighbors), linear (all OH groups have two neighbors, except two that have only one neighbor) and ramified or lasso (when at least an OH group has more than two neighbors).

Figure 6 shows the probability distribution for finding a molecule in an aggregate of a given size and type (linear, cyclic, and branched). The first general observation is that the 1*H*,1*H*-perfluorinated alcohols display a very rich aggregation behavior. On average, only 3−5% of molecules are found as monomers. Aggregates of 4 to 10 molecules are the most frequent, of any type, although aggregates of all sizes can be found. The relative frequency of small aggregates (dimers, trimers, and tetramers) decreases with the size of the alcohol, whereas larger aggregates become more frequent as the chain length increases. This enhancement of the tendency to form large aggregates is especially clear for the aggregates with 50 or

https://doi.org/10.1021/acs.jced.2c00410
J. Chem. Eng. Data XXXX, XXX, XXX−XXX

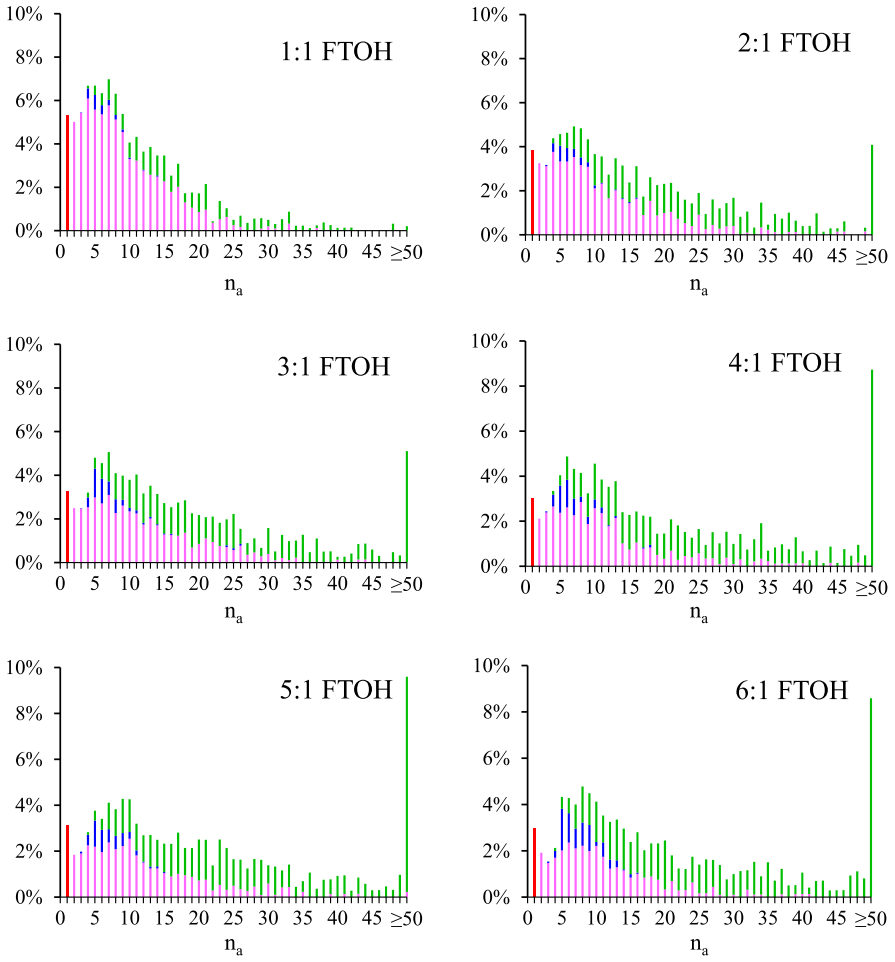

Figure 6. Percentage distribution of OH groups in monomers (red ■), linear (pink ■), cyclic (blue ■), and branched (green ■) aggregates, as a function of the aggregate size (n_a) for 1:1 FTOH, 2:1 FTOH, 3:1 FTOH, 4:1 FTOH, 5:1 FTOH, and 6:1 FTOH, obtained from MD simulations performed at 298.15 K and 0.1 MPa.

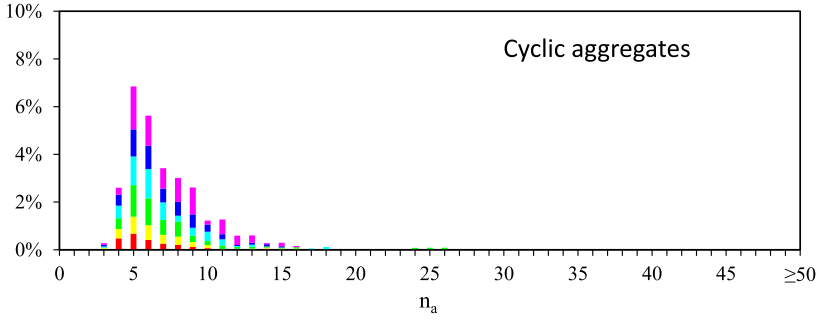

Figure 7. Frequency of cyclic aggregates as a function of the aggregate size (n_a) for 1:1 FTOH (red ■), 2:1 FTOH (yellow ■), 3:1 FTOH (green ■), 4:1 FTOH (aqua blue ■), 5:1 FTOH (blue ■), and 6:1 FTOH (pink ■) from MD simulations at 298.15 K and 0.1 MPa.

more molecules, which are almost nonexistent in 1:1 FTOH but increase in importance along the chemical family, accounting for around 9% of the total molecules for 4:1 FTOH and the larger alcohols. The maximum aggregation numbers observed also seem to increase with the chain length of the alcohol and ranged from ∼60 for 1:1 FTOH to ∼150 for 6:1 FTOH. For all alcohols, a significant number of molecules form cyclic aggregates of size 4 and larger, but it is also evident that the importance of this type of aggregates increases with the size of the molecule. This is clearly illustrated in Figures 7 and 8. A possible interpretation is that as the chain length increases, the hydroxyl groups become progressively more "diluted", making the formation of linear aggregates less probable. The formation of cyclic "reverse micelle-like" aggregates maximizes the total number of hydrogen bonds, thus reducing the configurational energy of the system. Similarly, the formation of branched aggregates, in which an alcohol molecule makes more than two hydrogen bonds, also increases the total number of hydrogen bonds and, as can be seen, this type of aggregate also becomes more frequent as the chain length increases.

https://doi.org/10.1021/acs.jced.2c00410
J. Chem. Eng. Data XXXX, XXX, XXX−XXX

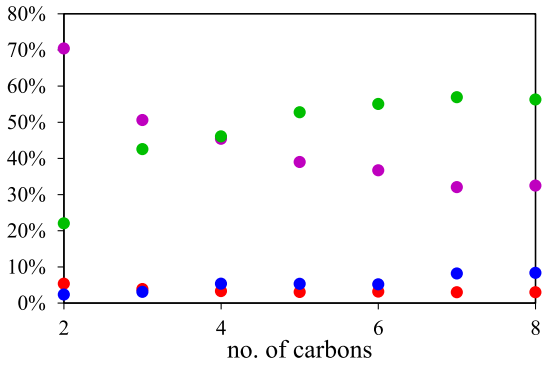

Figure 8. Percentage of monomers (red ●), linear (violet ●), cyclic (blue ●), and branched (green ●) aggregates, as a function of chain length of the 1*H*,1*H*-perfluorinated alcohols from MD simulations at 298.15 K and 0.1 MPa.

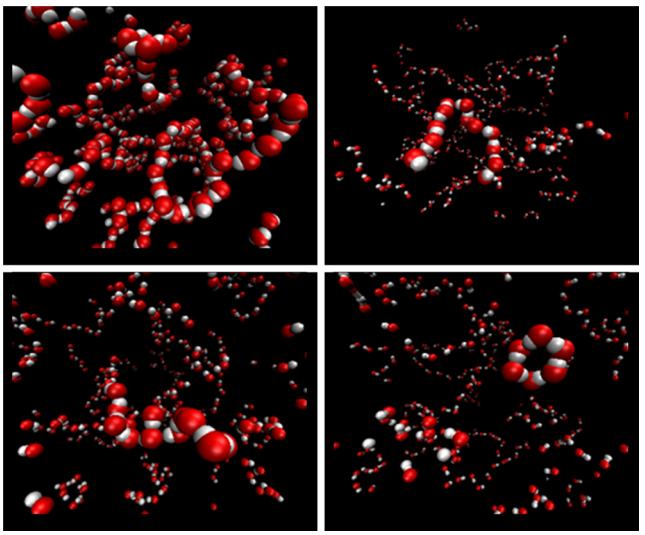

Figure 9. MD simulation snapshots of 1*H*,1*H*-perfluorohexanol at 298.15 K and 1 atm, illustrating the full H-bond network (top left) and emphasizing the different types of aggregates: linear (top right), branched (bottom left), and cyclic (bottom right). Perfluorinated chains are omitted to allow visualization of the O···OH network; the oxygen atom is represented in red, and the hydrogen atom is represented in white.

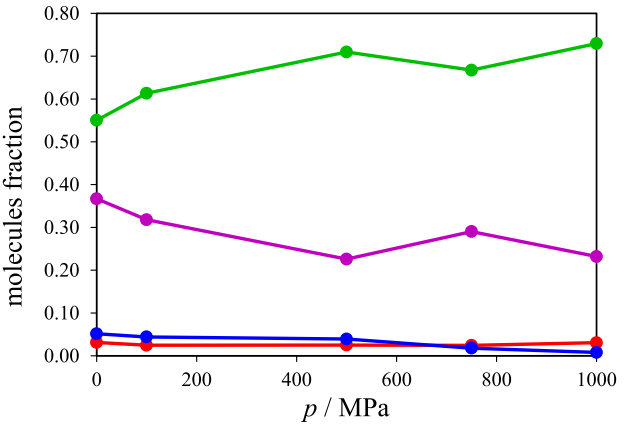

Figure 11. Fraction of molecules involved in different types of aggregates [monomers (red ●), linear (violet ●), cyclic (blue ●), and branched (green ●)] as a function of pressure for 1*H*,1*H*-perfluorohexanol at 298.15 K.

Figure 9 shows MD simulation snapshots of 1*H*,1*H*-perfluorohexanol at 298.15 K and 1 atm, illustrating the H-bond network and emphasizing the different types of aggregate: linear, branched, and cyclic. The perfluorinated chains have been omitted to visually emphasize the O···HO network.

The effect of pressure on the organization of the liquids was also tested and analyzed by MD. Simulations were performed for the different alcohols at several pressures, between 0.1 MPa and 1 GPa, at constant temperature. The simulation results were found to be equivalent for all the studied alcohols; thus, only those for 1*H*,1*H*-perfluorohexanol are presented. Figure 10 displays the radial distribution functions (rdfs) for selected atom pairs, namely, between the oxygen atom and the hydroxyl hydrogen of neighbor molecules (Figure 10a) and between terminal CF_3 groups (Figure 10b). The first provides information on the effect of pressure on the H-bonded molecules. As can be seen, increasing pressure slightly reduces the intensity of both O−H peaks, although by a very small amount. The effect of pressure on H-bonds is thus very small. As for the effect of pressure on the packing of the perfluorinated chains, this can be assessed analyzing the rdfs between terminal CF_3 groups. In this case, the rdfs are practically indistinguishable as pressure increases, except for the higher pressures above 500 MPa, for which the rdfs are

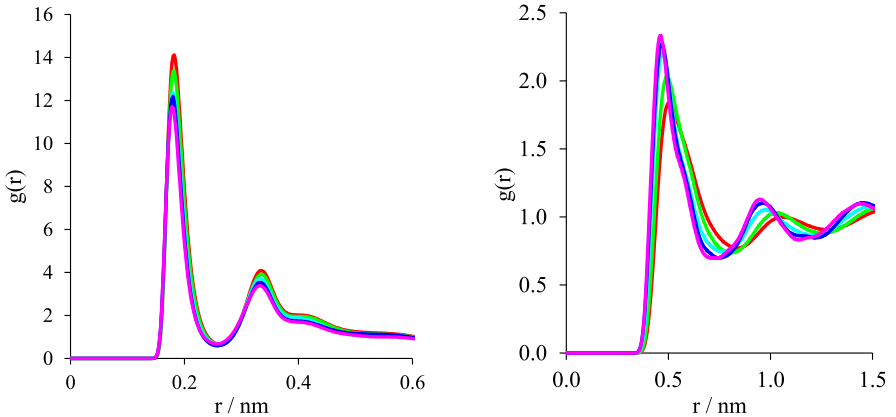

Figure 10. MD intermolecular rdfs between O−H (left) and CF_3−CF_3 (right) for 1*H*,1*H*-perfluorohexanol at 298.15 K and 0.1 MPa (red —), 100 MPa (green —), 500 MPa (aqua blue —), 750 MPa (blue —), and 1000 MPa (purple —).

https://doi.org/10.1021/acs.jced.2c00410
J. Chem. Eng. Data XXXX, XXX, XXX−XXX

gradually displaced to lower distances, indicating a tighter packing of the perfluorinated chains. Finally, the effect of pressure on the fraction of different types of aggregates can be observed in Figure 11. As can be seen, the influence of pressure on the fraction of monomers and cyclic aggregates is small. Conversely, the fraction of linear aggregates decreases with pressure, while that of branched aggregates increases. It should be realized, however, that these are extremely high pressures. Our experimental results do not exceed 70 MPa. Nevertheless, our results are in agreement with those reported by Mariani et al.,[41] who performed equivalent simulations for hydrogenated *n*-alkanols.

5. CONCLUSIONS

New experimental liquid densities as a function of pressure (0.1−70 MPa) and temperature (293.15−313.15 K) are reported for five liquid 1*H*,1*H*-perfluorinated alcohols ($CF_3(CF_2)_nCH_2OH$, n = 2, 3, 4, 5, 6). Derivative properties such as the isothermal compressibility and isobaric thermal expansivity coefficients were calculated from the experimental data and compared with that for hydrogenated alcohols from the literature. Atomistic MD simulations were performed, enabling a detailed molecular-level view on the organization of the liquid, in particular the H-bond network of the perfluorinated alcohols.

■ ASSOCIATED CONTENT

Supporting Information

The Supporting Information is available free of charge at https://pubs.acs.org/doi/10.1021/acs.jced.2c00410.

Description of the OPLS-AA force-field functions and all parameters used in this work; uncertainty estimation procedure; plot of potential energy and volume during equilibration time; and comparison between experimental density data and literature data (PDF)

Coordinate and topology (.gro and .itp) files for all substances (ZIP)

■ AUTHOR INFORMATION

Corresponding Author

Eduardo J. M. Filipe − *Centro de Química Estrutural, Institute of Molecular Sciences, Departamento de Engenharia Química, Instituto Superior Técnico, Universidade de Lisboa, 1049-001 Lisboa, Portugal;* orcid.org/0000-0003-4440-7710; Email: efilipe@tecnico.ulisboa.pt

Authors

Diogo Machacaz − *Centro de Química Estrutural, Institute of Molecular Sciences, Departamento de Engenharia Química, Instituto Superior Técnico, Universidade de Lisboa, 1049-001 Lisboa, Portugal;* orcid.org/0000-0003-3803-4882

Tiago M. Eusébio − *Centro de Química Estrutural, Institute of Molecular Sciences, Departamento de Engenharia Química, Instituto Superior Técnico, Universidade de Lisboa, 1049-001 Lisboa, Portugal*

Cátia Guarda − *Centro de Química Estrutural, Institute of Molecular Sciences, Departamento de Engenharia Química, Instituto Superior Técnico, Universidade de Lisboa, 1049-001 Lisboa, Portugal*

Gonçalo M. C. Silva − *Centro de Química Estrutural, Institute of Molecular Sciences, Departamento de Engenharia Química, Instituto Superior Técnico, Universidade de Lisboa, 1049-001 Lisboa, Portugal*

Pedro Morgado − *Centro de Química Estrutural, Institute of Molecular Sciences, Departamento de Engenharia Química, Instituto Superior Técnico, Universidade de Lisboa, 1049-001 Lisboa, Portugal*

Luís F. G. Martins − *Centro de Química Estrutural, Institute of Molecular Sciences, Departamento de Engenharia Química, Instituto Superior Técnico, Universidade de Lisboa, 1049-001 Lisboa, Portugal; LAQV-REQUIMTE—Évora, Institute for Research and Advanced Studies, School of Science and Technology, University of Évora, 7000-671 Évora, Portugal;* orcid.org/0000-0001-7530-8606

José N. A. Canongia Lopes − *Centro de Química Estrutural, Institute of Molecular Sciences, Departamento de Engenharia Química, Instituto Superior Técnico, Universidade de Lisboa, 1049-001 Lisboa, Portugal;* orcid.org/0000-0002-4483-6294

Complete contact information is available at: https://pubs.acs.org/10.1021/acs.jced.2c00410

Notes

The authors declare no competing financial interest.

■ ACKNOWLEDGMENTS

Centro de Química Estrutural, Institute of Molecular Sciences, acknowledges funding from Fundação para a Ciência e a Tecnologia (FCT) through grants UIDB/00100/2020 and LA/P/0056/2020. LAQV-REQUIMTE, Évora pole, acknowledges financial support by National Funds through FCT within the scope of the project UIDB/50006/2020. T.M.E. acknowledges funding from FCT—Doctoral Programme in Nuclear Magnetic Resonance Applied to Chemistry, Materials and Biosciences−PTNMRPhD (PD/00065/2013), through grant no. PD/BD/147873/2019. G.M.C.S. and C.G. acknowledge funding from FCT, grant nos. SFRH/BD/123565/2016 and SFRH/BD/129589/2017.

■ REFERENCES

(1) Kissa, E.*Fluorinated Surfactants*; Marcel Dekker, Inc.: New York, 1993.

(2) Silva, G. M. C.; Morgado, P.; Haley, J. D.; Montoya, V. M. T.; McCabe, C.; Martins, L. F. G.; Filipe, E. J. M. Vapor Pressure and Liquid Density of Fluorinated Alcohols: Experimental, Simulation and GC-SAFT-VR Predictions. *Fluid Phase Equilib.* **2016**, *425*, 297−304.

(3) Silva, G. M. C.; Justino, J.; Morgado, P.; Teixeira, M.; Pereira, L. M. C.; Vega, L. F.; Filipe, E. J. M. Detailed Surface Characterization of Highly Fluorinated Liquid Alcohols: Experimental Surface Tensions, Molecular Simulations and Soft-SAFT Theory. *J. Mol. Liq.* **2020**, *300*, 112294.

(4) Pereira, L. A. M.; Martins, L. F. G.; Ascenso, J. R.; Morgado, P.; Ramalho, J. P. P.; Filipe, E. J. M. Diffusion Coefficients of Fluorinated Surfactants in Water: Experimental Results and Prediction by Computer Simulation. *J. Chem. Eng. Data* **2014**, *59*, 3151−3159.

(5) Martins, L. F. G.; Pereira, L. A. M.; Silva, G. M. C.; Ascenso, J. R.; Morgado, P.; Ramalho, J. P. P.; Filipe, E. J. M. Fluorinated Surfactants in Solution: Diffusion Coefficients of Fluorinated Alcohols in Water. *Fluid Phase Equilib.* **2016**, *407*, 322−333.

(6) Tomšič, M.; Jamnik, A.; Fritz-Popovski, G.; Glatter, O.; Vlček, L. Structural Properties of Pure Simple Alcohols from Ethanol, Propanol, Butanol, Pentanol, to Hexanol: Comparing Monte Carlo Simulations with Experimental SAXS Data. *J. Phys. Chem. B* **2007**, *111*, 1738−1751.

(7) Duarte, P.; Silva, M.; Rodrigues, D.; Morgado, P.; Martins, L. F. G.; Filipe, E. J. M. Liquid Mixtures Involving Hydrogenated and

Fluorinated Chains: (P, ρ, T,x) Surface of (Ethanol + 2,2,2-Trifluoroethanol), Experimental and Simulation. *J. Phys. Chem. B* **2013**, *117*, 9709−9717.
(8) Morgado, P.; Garcia, A. R.; Ilharco, L. M.; Marcos, J.; Anastácio, M.; Martins, L. F. G.; Filipe, E. J. M. Liquid Mixtures Involving Hydrogenated and Fluorinated Alcohols: Thermodynamics, Spectroscopy, and Simulation. *J. Phys. Chem. B* **2016**, *120*, 10091−10105.
(9) Silva, G. M. C.; Morgado, P.; Filipe, E. J. M. Towards Aqueous − Fluorous − Hydrogenous Emulsions: Phase Equilibria and Liquid Structure of (Water + 1H,1H-Perfluorobutanol + 1-Butanol) Ternary Mixture. *Fluid Phase Equilib.* **2020**, *522*, 112737.
(10) Isabel Cabaço, M. I.; Besnard, M.; Cruz, C.; Morgado, P.; Silva, G. M. C.; Filipe, E. J. M.; Coutinho, J. A. P.; Danten, Y. The Structure of Liquid Perfluoro Tert-Butanol Using Infrared, Raman and X-Ray Scattering Analyzed by Quantum DFT Calculations and Molecular Dynamics. *Chem. Phys. Lett.* **2021**, *779*, 138844.
(11) Cabaço, M. I.; Besnard, M.; Cruz, C.; Morgado, P.; Silva, G. M. C.; Filipe, E. J. M.; Coutinho, J. A. P.; Danten, Y. Breaking the Structure of Liquid Hydrogenated Alcohols Using Perfluorinated Tert -Butanol: A Multitechnique Approach (Infrared, Raman, and X-Ray Scattering) Analyzed by DFT and Molecular Dynamics Calculations. *J. Phys. Chem. B* **2022**, *126*, 1992−2004.
(12) Isabel Cabaço, M. I.; Besnard, M.; Morgado, P.; Filipe, E. J. M.; Coutinho, J. A. P.; Danten, Y. Gaseous Hetero Dimers of Perfluoro Tert-Butyl Alcohol with Hydrogenated Alcohols by Infrared Spectroscopy and Quantum DFT Calculations. *Chem. Phys.* **2021**, *544*, 111110.
(13) Benson, G. C.; Pflug, H. D. Molar Excess Volumes of Binary Systems of Normal Alcohols at 25.Deg. *J. Chem. Eng. Data* **1970**, *15*, 382−386.
(14) Morgado, P.; Rodrigues, H.; Blas, F. J.; McCabe, C.; Filipe, E. J. M. Perfluoroalkanes and Perfluoroalkylalkane Surfactants in Solution: Partial Molar Volumes in n-Octane and Hetero-SAFT-VR Modelling. *Fluid Phase Equilib.* **2011**, *306*, 76−81.
(15) Morgado, P.; Black, J.; Lewis, J. B.; Iacovella, C. R.; McCabe, C.; Martins, L. F. G.; Filipe, E. J. M. Viscosity of Liquid Systems Involving Hydrogenated and Fluorinated Substances: Liquid Mixtures of (Hexane+perfluorohexane). *Fluid Phase Equilib.* **2013**, *358*, 161−165.
(16) Morgado, P.; Garcia, A. R.; Martins, L. F. G.; Ilharco, L. M.; Filipe, E. J. M. Alkane Coiling in Perfluoroalkane Solutions: A New Primitive Solvophobic Effect. *Langmuir* **2017**, *33*, 11429−11435.
(17) Morgado, P.; Martins, L. F. G.; Filipe, E. J. M. From Nano-Emulsions to Phase Separation: Evidence of Nano-Segregation in (Alkane + Perfluoroalkane) Mixtures Using 129Xe NMR Spectroscopy. *Phys. Chem. Chem. Phys.* **2019**, *21*, 3742−3751.
(18) Lo Nostro, P. Phase Separation Properties of Fluorocarbons, Hydrocarbons and Their Copolymers. *Adv. Colloid Interface Sci.* **1995**, *56*, 245−287.
(19) de Gracia Lux, C. G.; Donnio, B.; Heinrich, B.; Krafft, M. P. Thermal Behavior and High- and Low-Temperature Phase Structures of Gemini Fluorocarbon/Hydrocarbon Diblocks. *Langmuir* **2013**, *29*, 5325−5336.
(20) Morgado, P.; Barras, J.; Filipe, E. J. M. From Nano-Seggregation to Mesophases: Probing the Liquid Structure of Perfluoroalkylalkanes with 129Xe NMR Spectroscopy. *Phys. Chem. Chem. Phys.* **2020**, *22*, 14736−14747.
(21) Bardin, L.; Faure, M. C.; Filipe, E. J. M.; Fontaine, P.; Goldmann, M. Highly Organized Crystalline Monolayer of a Semi-Fluorinated Alkane on a Solid Substrate Obtained by Spin-Coating. *Thin Solid Films* **2010**, *519*, 414−416.
(22) Silva, G. M. C.; Morgado, P.; Lourenço, P.; Goldmann, M.; Filipe, E. J. M. Spontaneous Self-Assembly and Structure of Perfluoroalkylalkane Surfactant Hemimicelles by Molecular Dynamics Simulations. *Proc. Natl. Acad. Sci. U.S.A* **2019**, *116*, 14868−14873.
(23) Costa, J. C. S.; Fulem, M.; Schröder, B.; Coutinho, J. A. P.; Monte, M. J. S.; Santos, L. M. N. B. F. Evidence of an Odd−Even Effect on the Thermodynamic Parameters of Odd Fluorotelomer Alcohols. *J. Chem. Thermodyn.* **2012**, *54*, 171−178.
(24) Wagner, W.; Pruß, A. The IAPWS Formulation 1995 for the Thermodynamic Properties of Ordinary Water Substance for General and Scientific Use. *J. Phys. Chem. Ref. Data* **2002**, *31*, 387.
(25) Cibulka, I.; Takagi, T. P−ρ−T Data of Liquids: Summarization and Evaluation. 5. Aromatic Hydrocarbons. *J. Chem. Eng. Data* **1999**, *44*, 411−429.
(26) Cibulka, I.; Takagi, T.; Růžička, K. P−ρ−T Data of Liquids: Summarization and Evaluation. 7. Selected Halogenated Hydrocarbons. *J. Chem. Eng. Data* **2001**, *46*, 2−28.
(27) Jorgensen, W. L.; Maxwell, D. S.; Tirado-Rives, J. Development and Testing of the OPLS All-Atom Force Field on Conformational Energetics and Properties of Organic Liquids. *J. Am. Chem. Soc.* **1996**, *118*, 11225−11236.
(28) Watkins, E. K.; Jorgensen, W. L. Conformational Analysis and Liquid-State Properties from Ab Initio and Monte Carlo Calculations. *J. Phys. Chem. A* **2001**, *105*, 4118−4125.
(29) Van Der Spoel, D.; Lindahl, E.; Hess, B.; Groenhof, G.; Mark, A. E.; Berendsen, H. J. C. GROMACS: Fast, Flexible, and Free. *J. Comput. Chem.* **2005**, *26*, 1701−1718.
(30) Dymond, J. H.; Malhotra, R. The Tait Equation: 100 Years On. *Int. J. Thermophys.* **1988**, *9*, 941−951.
(31) Nakazawa, N.; Sako, T.; Nakane, T.; Sekiya, A.; Sato, M.; Gotoh, Y.; Suga, A. Densities and viscosities of fluorinated alcohols and fluorinated ethers. *Kagaku Kogaku Ronbunshu* **1996**, *22*, 184−189.
(32) Matsuo, S.; Yamamoto, R.; Kubota, H.; Tanaka, Y. Volumetric properties of mixtures of fluoroalcohols and water at high pressures. *Int. J. Thermophys.* **1994**, *15*, 245−259.
(33) Denda, M.; Touhara, H.; Nakanishi, K. Excess molar enthalpies for (water + a fluoroalkanol). *J. Chem. Thermodyn.* **1987**, *19*, 539−542.
(34) Johnson, R. E., Jr.; Dettre, R. H. The wettability of low-energy liquid surfaces. *J. Colloid Interface Sci.* **1966**, *21*, 610−622.
(35) Rochester, C. H.; Symonds, J. R. Thermodynamic Studies of Fluoroalcohols. Part I. Vapour Pressures and Enthalpies of Vaporization. *J. Chem. Soc., Faraday Trans. 1* **1973**, *69*, 1267−1273.
(36) Hashemi, H.; Nelson, W. M.; Babaee, S.; Naidoo, P.; Ramjugernath, D. Isothermal Vapor-Liquid Equilibrium Data for the Binary Systems Consisting of 1,1,2,3,3,3-Hexafluoro-1-propene and Either Methylcyclohexane, Cyclohexane, n-Hexane, 2-Methyltetrahydrofuran, or 2,2,3,3,4,4,4-Heptafluoro-1-butanol. *J. Chem. Eng. Data* **2019**, *64*, 5232−5237.
(37) Cibulka, I. Saturated Liquid Densities of 1-Alkanols from C1 to C10 and n-Alkanes from C5 to C16: A Critical Evaluation of Experimental Data. *Fluid Phase Equilib.* **1993**, *89*, 1−18.
(38) Cibulka, I.; Zikova, M. Liquid Densities at Elevated Pressures of 1-Alkanols from C1 to C10: A Critical Evaluation of Experimental Data. *J. Chem. Eng. Data* **1994**, *39*, 876−886.
(39) Wolfe, S. Gauche effect. Stereochemical Consequences of Adjacent Electron Pairs and Polar Bonds. *Acc. Chem. Res.* **1972**, *5*, 102−111.
(40) Padró, J. A.; Saiz, L.; Guàrdia, E. Hydrogen Bonding in Liquid Alcohols: A Computer Simulation Study. *J. Mol. Struct.* **1997**, *416*, 243−248.
(41) Mariani, A.; Ballirano, P.; Angiolari, F.; Caminiti, R.; Gontrani, L. Does High Pressure Induce Structural Reorganization in Linear Alcohols? A Computational Answer. *ChemPhysChem* **2016**, *17*, 3023−3029.

https://doi.org/10.1021/acs.jced.2c00410
J. Chem. Eng. Data XXXX, XXX, XXX−XXX